


## Article

# Oncolytic BHV-1 Is Sufficient to Induce Immunogenic Cell Death and Synergizes with Low-Dose Chemotherapy to Dampen Immunosuppressive T Regulatory Cells

Maria Eugenia Davola <sup>1</sup>, Olga Cormier <sup>1</sup>, Alyssa Vito <sup>1</sup>, Nader El-Sayes <sup>1</sup>, Susan Collins <sup>1</sup>, Omar Salem <sup>1</sup>, Spencer Revill <sup>1,2</sup>, Kjetil Ask <sup>1,2</sup>, Yonghong Wan <sup>1</sup> and Karen Mossman <sup>1,\*</sup> 

<sup>1</sup> Department of Medicine, Centre for Discovery in Cancer Research, McMaster University, Hamilton, ON L8S 4K1, Canada

<sup>2</sup> Firestone Institute for Respiratory Health, St. Joseph's Healthcare Hamilton, Hamilton, ON L8N 4A6, Canada

\* Correspondence: mossk@mcmaster.ca; Tel.: +1-905-525-9140 (ext. 23542)

**Simple Summary:** Immunotherapy is designed to stimulate the patient's own immune system to fight their specific cancer. While immune checkpoint therapies work well for some tumors, they fail to work in tumors that are "immune cold". Oncolytic viruses are viruses that preferentially target tumor cells while sparing healthy cells and can help stimulate immune responses. An oncolytic virus based on a common human herpesvirus has been granted FDA approval, and is currently being used as an intralesional cancer immunotherapy. We have previously shown that a related bovine herpesvirus has many unique properties that suggest widespread use against many types of primary and metastatic cancers. Here, we show for the first time in an immune competent mouse model that oncolytic BHV-1 can activate a type of immune response that can turn "cold" tumors "hot". Addition of low-dose chemotherapy to oncolytic BHV-1 increases good immune responses while decreasing harmful immune responses, allowing immune checkpoint therapy to clear tumors.



**Citation:** Davola, M.E.; Cormier, O.; Vito, A.; El-Sayes, N.; Collins, S.; Salem, O.; Revill, S.; Ask, K.; Wan, Y.; Mossman, K. Oncolytic BHV-1 Is Sufficient to Induce Immunogenic Cell Death and Synergizes with Low-Dose Chemotherapy to Dampen Immunosuppressive T Regulatory Cells. *Cancers* **2023**, *15*, 1295. <https://doi.org/10.3390/cancers15041295>

Academic Editor: Constantin N. Baxevanis

Received: 18 January 2023

Revised: 8 February 2023

Accepted: 13 February 2023

Published: 17 February 2023



**Copyright:** © 2023 by the authors. Licensee MDPI, Basel, Switzerland. This article is an open access article distributed under the terms and conditions of the Creative Commons Attribution (CC BY) license (<https://creativecommons.org/licenses/by/4.0/>).

**Abstract:** Immunogenic cell death (ICD) can switch immunologically "cold" tumors "hot", making them sensitive to immune checkpoint inhibitor (ICI) therapy. Many therapeutic platforms combine multiple modalities such as oncolytic viruses (OVs) and low-dose chemotherapy to induce ICD and improve prognostic outcomes. We previously detailed many unique properties of oncolytic bovine herpesvirus type 1 (oBHV) that suggest widespread clinical utility. Here, we show for the first time, the ability of oBHV monotherapy to induce bona fide ICD and tumor-specific activation of circulating CD8<sup>+</sup> T cells in a syngeneic murine model of melanoma. The addition of low-dose mitomycin C (MMC) was necessary to fully synergize with ICI through early recruitment of CD8<sup>+</sup> T cells and reduced infiltration of highly suppressive PD-1<sup>+</sup> Tregs. Cytokine and gene expression analyses within treated tumors suggest that the addition of MMC to oBHV therapy shifts the immune response from predominantly anti-viral, as evidenced by a high level of interferon-stimulated genes, to one that stimulates myeloid cells, antigen presentation and adaptive processes. Collectively, these data provide mechanistic insights into how oBHV-mediated therapy modalities overcome immune suppressive tumor microenvironments to enable the efficacy of ICI therapy.

**Keywords:** immunogenic cell death; oncolytic virus; bovine herpesvirus type 1; immune checkpoint inhibitors; mitomycin c; T regulatory cells

## 1. Introduction

Oncolytic viruses (OVs) are being actively studied as novel cancer therapeutics since they preferentially target and kill tumor cells and can stimulate an anti-tumor, patient-specific immune response [1]. Moreover, OVs can kill cancer stem cells and replicate in hypoxic environments and in drug-resistant cells [2,3]. While direct oncolysis was initially considered the primary mechanism of action of OVs, initiation of an anti-tumor immune

response is now considered an essential aspect of OV therapy [4,5]. Indeed, OVs are potent inducers of in situ vaccination, using the tumor as the antigen source for immune stimulation [6–8]. OVs turn “immune cold” tumors “immune hot”, allowing tumors to effectively respond to immune checkpoint inhibitor (ICI) therapy [9]. It is believed that OV-mediated initiation of host anti-tumor immunity is a result of the induction of immunogenic cell death (ICD) [10,11]. ICD then triggers innate and adaptive anti-tumor immune activation [12].

Combination platforms using OVs with low-dose chemotherapy have shown increased ICD induction over monotherapies alone with increased infiltration of CD8<sup>+</sup> T cells into tumors [13], therefore yielding greater potential for synergy with ICI [14–16]. Pre-clinical and clinical trials have validated OVs [17] with a herpes simplex virus type 1 (HSV-1)-based OV approved by the USA Food and Drug Administration (FDA) for the treatment of melanoma in 2015 [18]. However, clinical trials have also revealed the limitations of OVs [19]. The pre-existence of antibodies against human OVs or rapid seroconversion after OV administration accelerates virus neutralization, limiting viral delivery to the tumor [20]. Additionally, many OVs are restricted by mutations and/or expressed antigens in the tumor, limiting tumor targeting [19]. Thus, new strategies are required to overcome the current clinical challenges of OV-based therapies and improve their translative potential.

In this sense, bovine herpesvirus type 1 (BHV-1), a close relative of HSV-1, has exciting properties for clinical development. Unlike HSV-1, BHV-1 does not cause disease in humans or infect healthy human cells and is not neutralized by human serum [21], allowing for either intratumoral or intravenous delivery for the treatment of primary and metastatic cancers. In addition to targeting multiple cancer subtypes, similar to HSV-1, BHV-1 also targets immortalized cells, suggesting pre-neoplastic to overt cancer cell activity [21]. It further targets bulk and cancer-initiating tumor cells, regardless of tumor status or subtype [2]. Oncolytic BHV-1 expressing green fluorescent protein (oBHV) killed more human cancer cell lines from the NCI60 panel with greater killing capacity than an ICP0-null oncolytic HSV-1 [22]. Of clinical relevance, oBHV has a particular affinity for cancers with a high incidence of mutant KRAS [22], a negative therapeutic outcome predictor of hard-to-treat cancers such as lung, colorectal and pancreatic cancers. In the NCI60 panel, the multiplicity of infection (MOI) of oBHV used, but not replication level, correlated with the cell-killing capacity [22]. As with other non-human viruses being developed as OVs, a fulsome understanding of how BHV-1 behaves in vivo is critical to ensure patient safety.

In vivo studies of BHV-1 are limited due to the lack of syngeneic animal models [23–25]. While cotton rats are susceptible to BHV-1, they are a challenging model to work with and limited reagents are available [26]. Nevertheless, we have previously shown that oBHV, in combination with the methyltransferase inhibitor 5-Azacytidine, significantly decreased the incidence of secondary lesions with enhanced tumor cell clearance and evidence of immune cell infiltration in a tolerized cotton rat model of breast adenocarcinoma [27]. Standard murine models are unsuitable as murine cells lack BHV-1 entry receptors [24,25]. In this study, we used a modified B16 melanoma mouse model (B16-C10) [28] expressing nectin-1, a human receptor for BHV-1 entry [29,30], to further investigate oBHV anti-tumor immunostimulatory properties. We found that while oBHV alone is sufficient to induce bona fide ICD and induce the activation of circulating CD8<sup>+</sup> T cells and tumor-infiltrating lymphocytes (TILs), low-dose mitomycin (MMC) chemotherapy is required to enable ICI to significantly extend survival.

## 2. Materials and Methods

### 2.1. Cell Lines

Cell lines were maintained at 37 °C with 5% CO<sub>2</sub> in a medium supplemented with 1 mM L-glutamine. MDBK-derived CRIB cells [31] were obtained from Prof. Clinton Jones (Oklahoma State University, US) and cultured in Dulbecco’s modified Eagle’s medium (DMEM) supplemented with 5% fetal bovine serum (FBS). B16 control and B16-C10 cells [28], which are derived from B78H1 cells, were obtained from Prof. Gary Cohen

(University of Pennsylvania, US) and maintained in DMEM supplemented with 5% FBS, 100 U/mL penicillin–streptomycin and 250 µg/mL Geneticin (Gibco Cat# 10131035).

## 2.2. Oncolytic Virus

oBHV, a BHV-1 recombinant that expresses green fluorescent protein (GFP), was a kind gift from Dr. Günther Keil (Friedrich-Loeffler-Institut, Greifswald, Mecklenburg-Vorpommern, Germany) [32]. oBHV contains murine cytomegalovirus (CMV) promoter and enhanced GFP sequence in the glycoprotein *gI* locus, resulting in *gI* disruption. oBHV was propagated and titrated on CRIB cells. The virus preparations included sucrose cushion purified, and the purified virus was resuspended in PBS and stored at  $-80^{\circ}\text{C}$  [2].

## 2.3. Drug Preparation

Mitomycin c (MMC) stock powder (Sigma-Aldrich, St. Louis, MO, USA Cat# M4287) was stored at  $4^{\circ}\text{C}$  and dissolved in sterile water to a concentration of 2 mg/mL. MMC was freshly prepared for each experiment.  $\alpha$ -CTLA-4 and  $\alpha$ -PD-L1 antibodies (BioXCell Cat# BE0131 and BE0101, respectively) were diluted to 1 mg/mL with sterile PBS.

## 2.4. Tumor Regression Studies in Mice Bearing B16-C10 Tumors

Female C57Bl/6 mice were maintained at the McMaster University Central Animal Facility; procedures were performed in full compliance with the Canadian Council on Animal Care and approved by the Animal Research Ethics Board of McMaster University. Then, 6- to 8-week-old C57Bl/6 mice were subcutaneously implanted with  $5 \times 10^6$  B16-C10 cells resuspended in 200 µL PBS into the left flank [28]. Tumors reached palpable size ( $50\text{--}100\text{ mm}^3$ ) within 2 weeks of the injection (day 1). For MMC monotherapy, tumors were treated intratumorally (i.t.) with 100 µg MMC in 50 µL sterile water only at day 1. For oBHV monotherapy, tumors were treated i.t. by injecting  $2 \times 10^7$  pfu oBHV in 50 µL PBS once daily beginning at day 2 for three consecutive days (days 2, 3 and 4) [13,27]. For ICI monotherapy, tumors were treated with mouse  $\alpha$ -CTLA-4 and  $\alpha$ -PD-L1 antibodies intraperitoneally (i.p.) (200 µg each) from day 2 every 3 days until 10 doses total. For combinatorial therapies, tumors were treated with MMC or 50 µL sterile water i.t. at day 1, oBHV or 50 µL PBS i.t. at days 2, 3 and 4, and  $\alpha$ -CTLA-4 and  $\alpha$ -PD-L1 antibodies or 200 µL PBS from day 2 every 3 days until 10 doses total. Tumors were measured every 3–4 days using a digital caliper from day 1 until endpoint, when tumors reached a volume of  $525\text{ mm}^3$ .

## 2.5. Histology and Image Analysis

Treated and control tumors were resected and fixed in 10% formalin for 48 h and then transferred to 70% ethanol until histological processing. Tumor tissue was embedded in paraffin and 4-µm sections were prepared. Tissue sections were processed for immunohistochemistry (IHC) using Automated Leica Bond Rx stainer with Epitope Retrieval Buffer 2 (Leica, Wetzlar, Germany, AR9640). All antibodies were diluted in IHC/ISH Super Blocker (Leica, PV6199). Primary antibodies and working dilutions were as follows:  $\alpha$ -CD4 (1:800; Ebio) and  $\alpha$ -CD8a (1:1000; Ebio). Secondary antibody and working dilution: rabbit  $\alpha$ -rat antibody (1:100; Vector Labs). The Bond Refine Polymer detection kit (Leica, Concord, ON, Canada) was used.

Staining was digitalized using the Olympus VS120-L100-W automated slide scanner. Slides were batch-scanned on the brightfield setting at  $20\times$  magnification. The color camera used was the Pike 505C VC50. HALO Image Analysis Software (Indica Labs, HALO v2.2) was used to analyze digital histology images. Cytonuclear cell count algorithms were developed to determine the amount of CD4 and CD8a positive cells and total cell numbers in a given tissue sample. The percentage of positive cells was calculated relative to total cell number.

### 2.6. Gold Standard ICD Immunization Assay

Female C57Bl/6 mice were vaccinated with dying B16-C10 cells. B16-C10 cells were mock- or infected with oBHV at MOI of 20 for 1 h at 37 °C; the virus inoculum was removed, cells were washed with PBS and media were added back. After 2 h at 37 °C, the media were replaced with fresh media with or without 20 µg/mL MMC and cells were incubated for 14 h at 37 °C. The optimal timepoint for harvesting cells that were in the process of dying was chosen as the timepoint where cellular viability started to decrease compared to untreated cells (see Figure S1, 14 h post-infection). Treated cells and supernatant were harvested and centrifugated at 1000 rpm for 10 min at 4 °C. Pellets were resuspended in PBS and used for vaccination. Each mouse was vaccinated subcutaneously with only PBS (N = 8) (as carrier control) or  $3 \times 10^6$  cells (200 µL) (N = 10) on the left flank. Three days post-vaccination,  $5 \times 10^6$  B16-C10 cells were implanted on the right flank (challenge). Once palpable, tumors were measured every 3–4 days until endpoint.

### 2.7. Tumor-Specific Activation of Circulating CD8<sup>+</sup> T Cells

On day 7 post-treatment, blood was collected from the periorbital sinus of mice and red blood cells were lysed using ACK buffer. Peripheral blood mononuclear cells (PBMCs) were stimulated with a collection of tumor B16-associated peptides: gp70, gp100 and P15e (1 µg/mL) in the presence of brefeldin A (GolgiPlug; BD Pharmingen Cat# 555029, 1 µg/mL added after 1 h of incubation). After 5 h of incubation, cells were treated with α-CD16/CD32 (Fc block; BD Pharmingen Cat# 553142) and the surface stained with α-CD8a antibody (BD Pharmingen Cat# 552877). Cells were then permeabilized and fixed with cytofix/cytoperm (BD Pharmingen Cat# 554714) and stained for intracellular interferon γ (IFNγ) (BD Biosciences, Franklin Lakes, NJ, USA, Cat# 554410). Data were acquired using LSRFortessa flow cytometer with FACSDiva software (BD Pharmingen) and analyzed with FlowJo Mac, version 10.6 software (BD, Ashland, OR, USA).

### 2.8. Re-Challenge Experiment

Mice that completely responded to triple combination therapy (tumor-free mice) (N = 4) and naïve 6- to 8-week-old control mice (N = 10) were subcutaneously implanted with  $5 \times 10^6$  B16-C10 cells resuspended in 200 µL PBS into the right flank (opposite of initial tumor cell implantation). Once palpable, tumors were measured every 3–4 days for 4 weeks.

### 2.9. Flow Cytometry Analysis

Tumors were minced with a razor blade in RPMI media. Then, 50 µg/mL liberase (Sigma Aldrich Cat# 5401054001) was added for digestion and samples incubated for 20 min at 37 °C. The cell suspension was passed over a 100-micron filter and rinsed with 5 mL of RPMI. Samples were spun at 1500 rpm for 5 min. Red blood cells were lysed using ACK buffer. The PBMCs were treated with anti-CD16/CD32 (Fc block; BD Biosciences Cat# 553141) and the surface stained with fluorescently conjugated antibodies for FVS (BD Biosciences, #564406), CD3 (BD Biosciences Cat# 564010), CD4 (BD Biosciences Cat# 561830), CD8 (BD Biosciences Cat# 563046), PD-1 (BD Biosciences Cat# 748266), Tim-3 (BD Biosciences Cat# 747626), CD25 (BD Biosciences Cat# 563061), and FoxP3 (BD Biosciences Cat# 560403). LSRFortessa flow cytometer with FACSDiva software (BD Biosciences) was used for data acquisition and FlowJo Mac, version 10.8.1 software, was used for data analysis.

### 2.10. Cytokine Analysis

B16-C10 tumors were treated with PBS, oBHV or MMC + oBHV as described previously. On days 3 and 5, tumors were resected and cut into small pieces and homogenized in the presence of a tissue extraction solution (50 mM Tris, pH 7.4, 250 mM NaCl, 5 mM EDTA, 2 mM Na<sub>3</sub>VO<sub>4</sub>, 1 mM NaF, 20 mM Na<sub>4</sub>P<sub>2</sub>O<sub>7</sub>, 1 mM beta-glycerophosphate, 1% NP-40) [14]. Homogenized tumors were incubated on ice for 30 min. Whole-tumor lysates

were clarified using three sequential centrifugations at 14,000 rpm for 10 min at 4 °C. Tumor homogenates were diluted to achieve equal amounts of protein concentration. The 44-Plex murine cytokine/chemokine analysis was conducted by Eve Technologies (Calgary, AB, Canada).

### 2.11. Clariom S Assay Transcriptional Profiling

B16-C10 tumors were treated with PBS, oBHV or MMC + oBHV as described previously. Tumors were collected from mice on day 5 and homogenized in Trizol (Invitrogen, Life Technologies Corporation, Carlsbad, CA, USA). Following Trizol extraction, the RNA was further purified using the Qiagen RNA extraction kit (Cat #74004). Extracted RNA was diluted to a concentration of 100 ng/μL and underwent reverse transcription. sscDNA was purified using magnetic beads and fragmented using UDG. The fragmented sample was hybridized to the Affymetrix Clariom S mouse arrays, and the stained arrays were scanned to generate intensity data. All of the reagents for this assay were developed by and purchased from Thermo Fisher Scientific. Raw data were analyzed using the Thermo Fisher Transcriptome Analysis Console software, version 4.0.2.1.5. The complete dataset can be found in the GEO database, TBD.

### 2.12. Statistical Analysis

Student's *t*-test was used to compare two groups of data, while one-way ANOVA was performed to determine the difference among three or more groups. Kaplan–Meier curves were used to estimate survival, and the log-rank Mantel–Cox test and the Gehan–Breslow–Wilcoxon test were used to determine the difference in survival. The null hypothesis was rejected for *p*-values less than 0.05. All data analyses were carried out using GraphPad Prism.

## 3. Results

### 3.1. Use of B16-C10 Syngeneic Melanoma Model for Pre-Clinical Analysis of oBHV

While OV's display limited therapeutic efficacy as monotherapies, several studies have shown that OV's synergize with low-dose chemotherapies [13,15] at doses that exhibit immunomodulatory but not cytotoxic properties [33–35]. MMC has been studied extensively in the context of ICD [36–38] and with OV's, including oncolytic herpesviruses [39–42]. Here, we evaluated the therapeutic efficacy of oBHV alone or in combination with low-dose MMC. To overcome the lack of syngeneic mouse models susceptible to oBHV, we used B16-C10 cells [28], genetically engineered B16 mouse melanoma cells expressing nectin-1, a human BHV-1 entry receptor [29]. B16-C10 cells form tumors reproducibly in C57Bl/6 mice, and nectin-1 expression does not induce detectable *in vivo* immunogenicity against tumors [28]. *In vitro* results confirm that nectin-1 expression improves oBHV entry into B16 cells (Figure S2). However, oBHV replication in B16-C10 cells was very low as shown in Figure S3A, where it was compared to a highly productive OV, such as oncolytic HSV-1 (oHSV) [43].

C57Bl/6 mice bearing subcutaneous B16-C10 tumors were treated *i.t.* with PBS, three doses of oBHV ( $2 \times 10^7$  pfu each), one dose of MMC (100 μg) or the combination of MMC and oBHV, as shown in Figure 1A. Tumor volumes were monitored every 3–4 days until the mice reached endpoint. Although neither oBHV nor MMC showed efficacy as monotherapies, their combination slightly slowed tumor growth (Figure 1B), though without a significant increase in survival (Figure 1C). The lack of efficacy of oBHV monotherapy is not related with its low-productive replication *in vitro* in B16-C10, as a highly productive oHSV also failed as monotherapy (Figure S3B). Of interest, MMC failed to enhance oBHV low-productive replication *in vitro*. In contrast, MMC significantly dampened the production of *de novo* virus (Figure S4A) but kept B16-C10 viability at levels comparable to those of MMC alone (Figure S4B). To investigate the immune landscape of untreated and treated B16-C10 tumors, a histologic assessment was performed. Tumors were harvested on days 7 and 10 from mice treated with PBS, oBHV, MMC or MMC + oBHV, and stained with

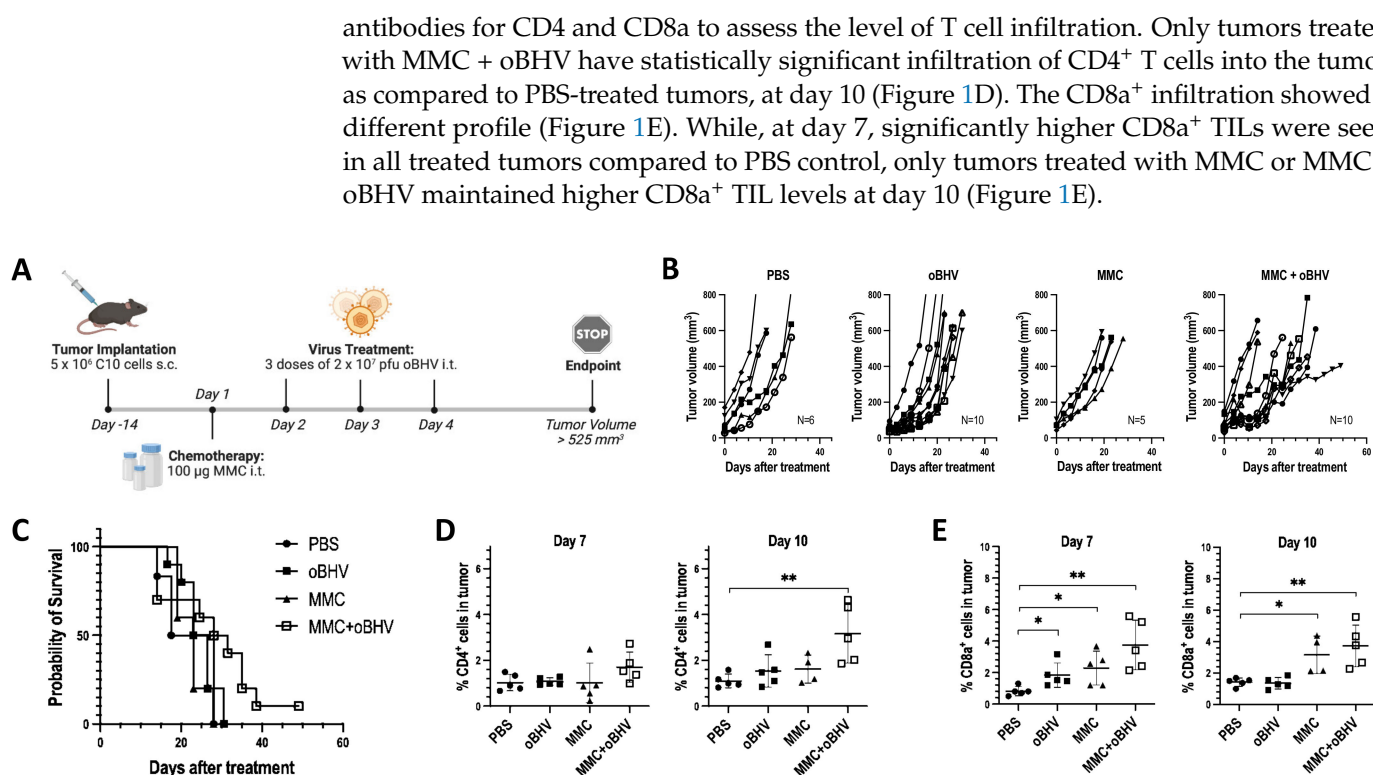


**Figure 1.** B16-C10 tumors were treated with PBS, oBHV, MMC or combination of MMC and oBHV (MMC + oBHV) (A). Tumors were measured every 3–4 days until animals reached endpoint. Tumor volume progression of each mice in each group (B) and Kaplan–Meier survival curve (C) are shown. Tumors were harvested on days 7 and 10 and histologic assessment with antibodies for CD4 and CD8a was performed to assess the level of T cell infiltration across the treatment groups. Quantification of CD4 (D) and CD8a (E) stains were performed over the whole tumor area. \*  $p < 0.05$  and \*\*  $p < 0.01$ .

### 3.2. oBHV Alone Is Sufficient to Induce ICD and Tumor-Specific CD8<sup>+</sup> T Cell Activation

The mounting of a systemic anti-tumor immune response can be partially explained by the ability of therapies such as OVIs to induce ICD of cancer cells [10,11]. The gold standard assay to assess bona fide ICD uses dying tumor cells as a vaccine to determine if the type of cell death is sufficient to induce an immune response capable of limiting or controlling subsequent tumor formation [44]. Our group has published that oncolytic HSV-1 requires low-dose MMC, a non-ICD-inducer per se [36], to induce bona fide ICD and recruit TILs [14,16]. To further understand if oBHV also needs MMC to induce ICD and trigger T cell infiltration into the tumor, dying B16-C10 cells infected with oBHV or infected and treated with MMC (MMC + oBHV) were used to vaccinate naïve mice (Figure 2A). Conditions were determined as being sufficient to initiate cell death (Figure S1). As a negative control of ICD, a group of mice received only PBS (carrier, no cells), and another group received cells that were treated only with MMC (non-ICD-inducer).

As expected, vaccination with dying cells treated with MMC alone fails to limit tumor progression compared to the PBS (no cell) control, confirming the inability of MMC to kill B16-C10 cells in an immunogenic manner (Figure 2B). In contrast, vaccination with dying cells infected with oBHV alone was as effective as MMC + oBHV in limiting tumor growth (Figure 2B). Additionally, both killing methods of B16-C10 cells showed comparable efficacy as infected-cell vaccines for the treatment of mice bearing B16-C10 tumors (Figure S5). These data suggest that oBHV alone is sufficient to induce bona fide ICD of B16-C10 cells. Of interest, while MMC + oBHV increases cell death in vitro compared to oBHV alone (2 days post-infection, Figure S1), it does not increase the immunogenicity of dying cells (Figure 2B).

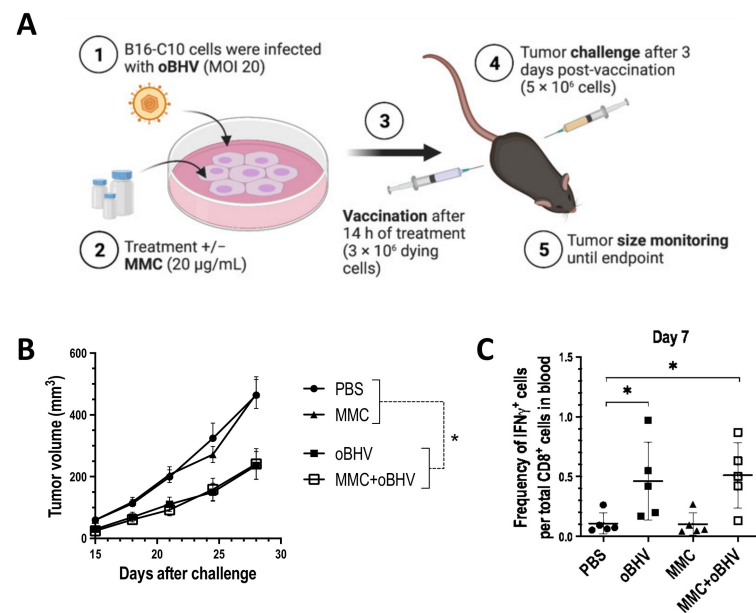


**Figure 2.** (A) B16-C10 cells were mock- or infected with oBHV (1) and, after 2 h, they were treated with or without MMC (2). After 14 h incubation, dying cells were used to vaccinate mice (3) and, 3 days later, untreated B16-C10 cells were implanted (challenge) (4). (5) Tumor volumes were measured from day 15 after challenge every 3–4 days until endpoint. (B) Tumors volume mean  $\pm$  SEM. (C) On day 7, blood was collected for IFN $\gamma$  intracellular staining of CD8 $^+$  T cells stimulated with tumor-specific peptides. \*  $p < 0.05$ .

ICD releases immunogenic molecules and tumor-associated antigens (TAAs), activating antigen-presenting cells (APCs) leading to the activation and recruitment of TILs [45,46]. The activation of circulating CD8 $^+$  T cells in tumor-bearing mice treated with PBS, MMC, oBHV or MMC + oBHV was evaluated on day 7 via IFN- $\gamma$  ICS of CD8 $^+$  T cells. Consistent with the bona fide ICD assay, only oBHV (with or without MMC), induced significant tumor-specific activation of circulating CD8 $^+$  T cells (Figure 2C).

### 3.3. Low-Dose MMC Synergizes with oBHV to Sensitize Tumors to ICI and Induce Long-Term Protective Immunity

We previously reported that the combination of low-dose MMC with oncolytic HSV-1 induced ICD and increased TILs, thus sensitizing tumors to ICI therapy [14,16]. Given that oBHV alone is sufficient to induce ICD and increase TILs, we hypothesized that oBHV monotherapy would sensitize tumors to ICI. Mice bearing B16-C10 tumors were treated with PBS, a mix of anti-PD-L1 and anti-CTLA-4 antibodies (ICI), oBHV + ICI, MMC + ICI, or the triple combination MMC + oBHV + ICI, as shown in Figure 3A. ICI alone failed to control tumor growth reflecting the immune “coldness” of the B16-C10 model (Figure 3B). While the combinations oBHV + ICI and MMC + ICI showed partial tumor control over PBS (Figure 3B), no significant increase in survival was observed (Figure 3C). The triple combination therapy, however, demonstrated enhanced tumor control (Figure 3B) and a significant increase in overall survival with 70% animal survival (Figure 3C) and 40% complete remission at day 49 after treatment (data not shown). Mice that fully responded to triple combination therapy (tumor-free mice) were re-challenged at day 56 via subcutaneous injection of B16-C10 cells into the opposite flank. All tumor-free mice rejected the second round of tumor engraftment (Figure 3D), suggesting a systemic long-term immune response against the tumor.

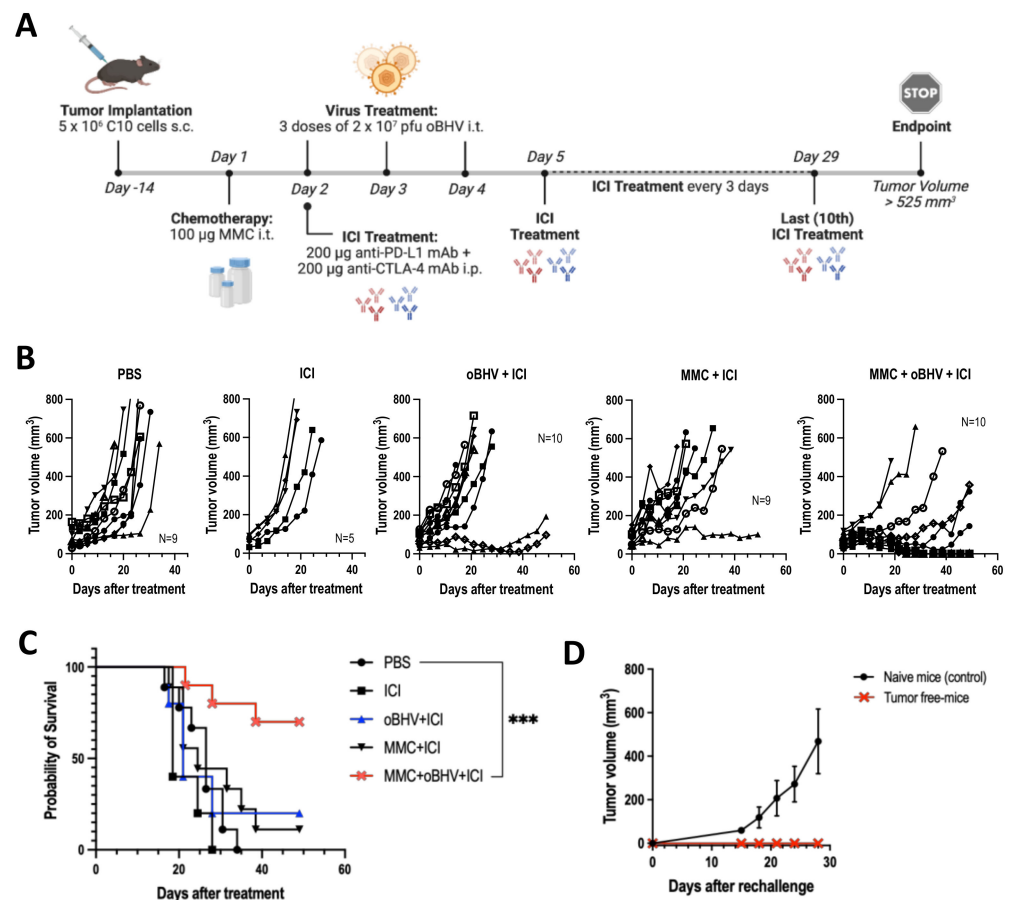


**Figure 3.** Tumors were treated with PBS, ICI ( $\alpha$ CTLA-4 &  $\alpha$ PD-L1) or different combinations of MMC, oBHV and ICI (A). Tumors were measured every 3–4 days until animals reached endpoint. Tumor volume progression of each mice in each group (B) and Kaplan-Meier survival curve (C) are shown. (D) Tumor-free mice that completely responded to MMC + oBHV + ICI treatment and naive mice (control) were re-challenged by B16-C10 implantation. Tumors were measured every 3–4 days for 4 weeks. Tumor volume mean  $\pm$  SEM is shown (D). \*\*\*  $p < 0.001$ .

### 3.4. Therapeutic Efficacy of Triple Combination Correlates with Early Tumor Infiltration of CD8<sup>+</sup> T Cells and Reduced Tumor Infiltration of Highly Suppressive PD-1<sup>+</sup> Treg Cells

To further investigate TIL distribution in treated mice, a histologic assessment was performed. Tumors treated with PBS, ICI, oBHV + ICI and the triple combination of MMC + oBHV + ICI were harvested at days 7 and 10 and stained with antibodies for CD8a and CD4. The localization of CD8a<sup>+</sup> (Figure 4A) and CD4<sup>+</sup> (Figure 5A) T cells was analysed, and their percentages were quantified (Figures 4B and 5B, respectively). As shown in Figure 4A, the distribution of CD8a<sup>+</sup> T cells in the tumor periphery on day 7 was clear after both ICI and oBHV + ICI treatments, but a visibly larger number of CD8a<sup>+</sup> T cells that infiltrated deep into the tumor tissue was observed with the triple combination. Tumors analyzed from day 10 show that oBHV + ICI-treated mice had comparable levels of recruitment (periphery) and infiltration (core) of cytotoxic T cells compared to triple-combination-treated mice (Figure 4A). Quantification shows that ICI, oBHV + ICI and MMC + oBHV + ICI significantly increased the percentage of CD8a<sup>+</sup> TILs compared to PBS at day 7, with the triple combination inducing the highest levels (Figure 4B). By day 10, tumors treated with oBHV + ICI had similar levels of CD8a<sup>+</sup> TILs compared to those with triple combination treatment (Figure 4B).

In addition, blood was collected at day 7 for IFN- $\gamma$  ICS of CD8<sup>+</sup> T cells stimulated with tumor-specific peptides (Figure 4C), and directly compared with tumor volumes to correlate levels of CD8<sup>+</sup> T cell activation with tumor growth (Figure 4D). Mice treated



with oBHV + ICI showed a high level of activation of circulating CD8<sup>+</sup> T cells, which was minimally impacted by the addition of MMC (Figure 4C). However, the addition of MMC was clearly necessary to control tumor growth (Figure 4D), with activated CD8<sup>+</sup> T cell levels within individual mice (indicated as a through f) failing to correlate with tumor control (Figure 4C,D).

The lack of correlation between day 10 CD8a<sup>+</sup> TILs and therapeutic efficacy could potentially be explained by differential cytotoxic T cell (Tc) exhaustion. Tumors treated with PBS, oBHV + ICI or triple combination were processed on day 10 and Tc were stained for two well-known exhaustion markers, PD-1 (Figure 4E) and TIM-3 (Figure 4F), for analysis via flow cytometry. However, no significant differences of Tc exhaustion were observed between treatments (Figure 4E,F). Of interest, both oBHV + ICI and triple combination were able to significantly reduce PD-1<sup>+</sup> Tc levels (Figure 4E) compared to PBS control.

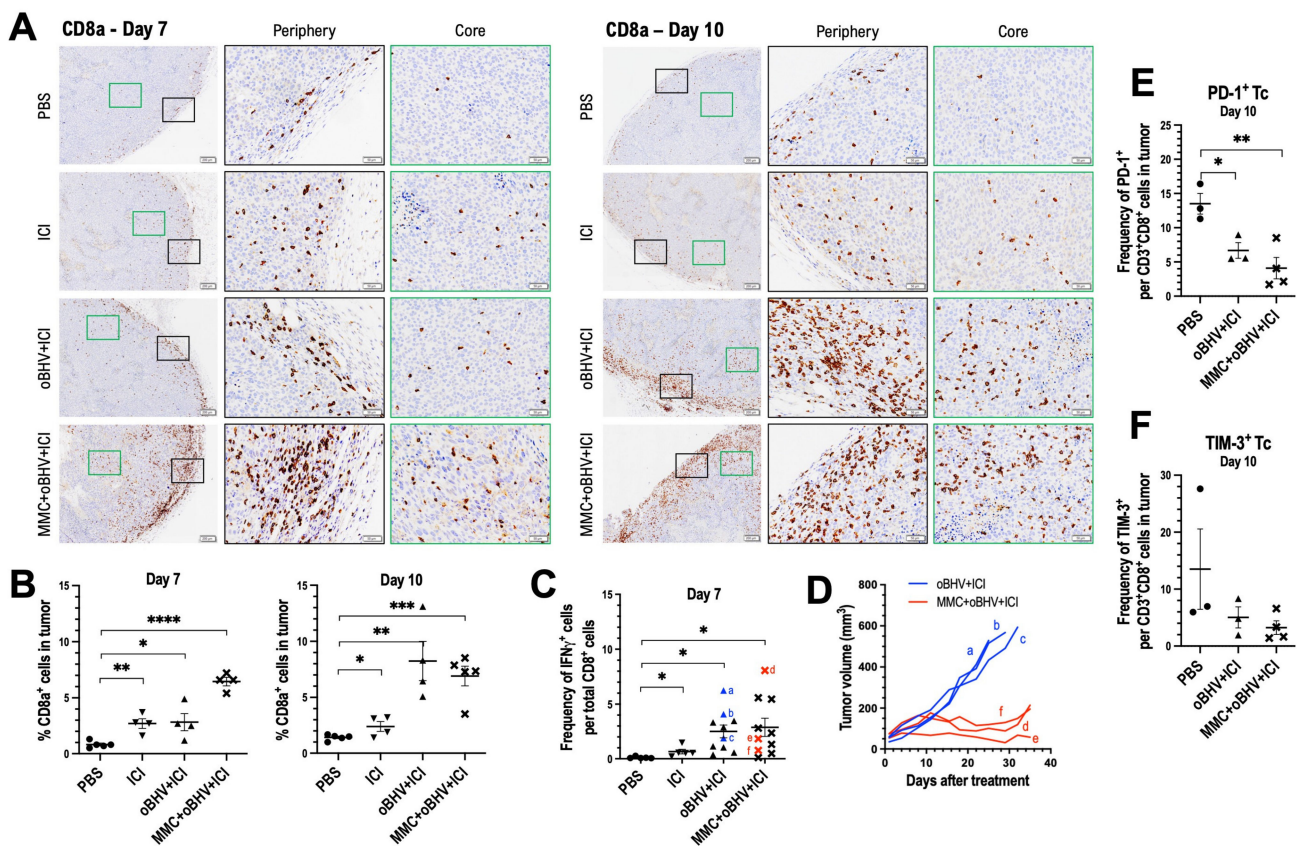


**Figure 4.** B16-C10 tumors were treated with PBS, ICI, oBHV + ICI or MMC + oBHV + ICI. CD8a IHC was performed on tumors on days 7 and 10 (A). Images with 2 $\times$  magnification are shown in left panels, and 10 $\times$  images of the tumor periphery (black) and core (green) are shown in the center and right panels. Scale bars: 200  $\mu$ m (left panels); 50  $\mu$ m (center and right panels). Quantification of CD8a<sup>+</sup> cells was performed over the whole tumor area (B). On day 7, blood was collected for IFN $\gamma$  ICS of peptide-stimulated CD8<sup>+</sup> T cells (C). Mice shown as red and blue dots identified with letters a–f in C were monitored for tumor growth (D). To evaluate the level of exhaustion of CD8<sup>+</sup> TILs (Tc) on day 10, tumors were processed and TILs were stained for analysis via flow cytometry (E,F). \*  $p < 0.05$ , \*\*  $p < 0.01$ , \*\*\*  $p < 0.001$ , \*\*\*\*  $p < 0.0001$ .

Although CD8<sup>+</sup> T cells are the most studied effector cells of cancer immunotherapy, CD4<sup>+</sup> T cells are also required for mounting an efficient anti-tumor immune response. On day 7, while CD4<sup>+</sup> T cells are observed in the periphery and core following all treatments (Figure 5A), the quantification indicated a significant increase only after combination treatments as compared to PBS-treated mice (Figure 5B). This significant increase in tumor-infiltrating CD4<sup>+</sup> T cells was maintained at day 10 (Figure 5B). However, as shown in

Figure 5A, a larger number of CD4<sup>+</sup> T cells was found in the periphery and core of oBHV + ICI-treated tumors. Interestingly, the addition of MMC to oBHV + ICI treatment clearly decreased the number of CD4<sup>+</sup> T cells both in the periphery and the core of tumors (Figure 5A).

To further investigate the difference in CD4<sup>+</sup> TIL levels, treated tumors were harvested and processed on day 10, and CD4<sup>+</sup> TILs were stained with CD25 and FoxP3 antibodies for flow cytometry analysis of Tregs. Triple combination therapy, but not oBHV + ICI, significantly reduced the proportion of CD25<sup>+</sup> FoxP3<sup>+</sup> Tregs among CD4<sup>+</sup> T cells (Figure 5C) and increased the Tc:Treg ratio (Figure 5D). Only the triple combination treatment was able to reduce the proportion of highly suppressive PD-1<sup>+</sup> Tregs (Figure 5E), while both combination treatments significantly reduced the TIM-3<sup>+</sup> Treg population (Figure 5F).

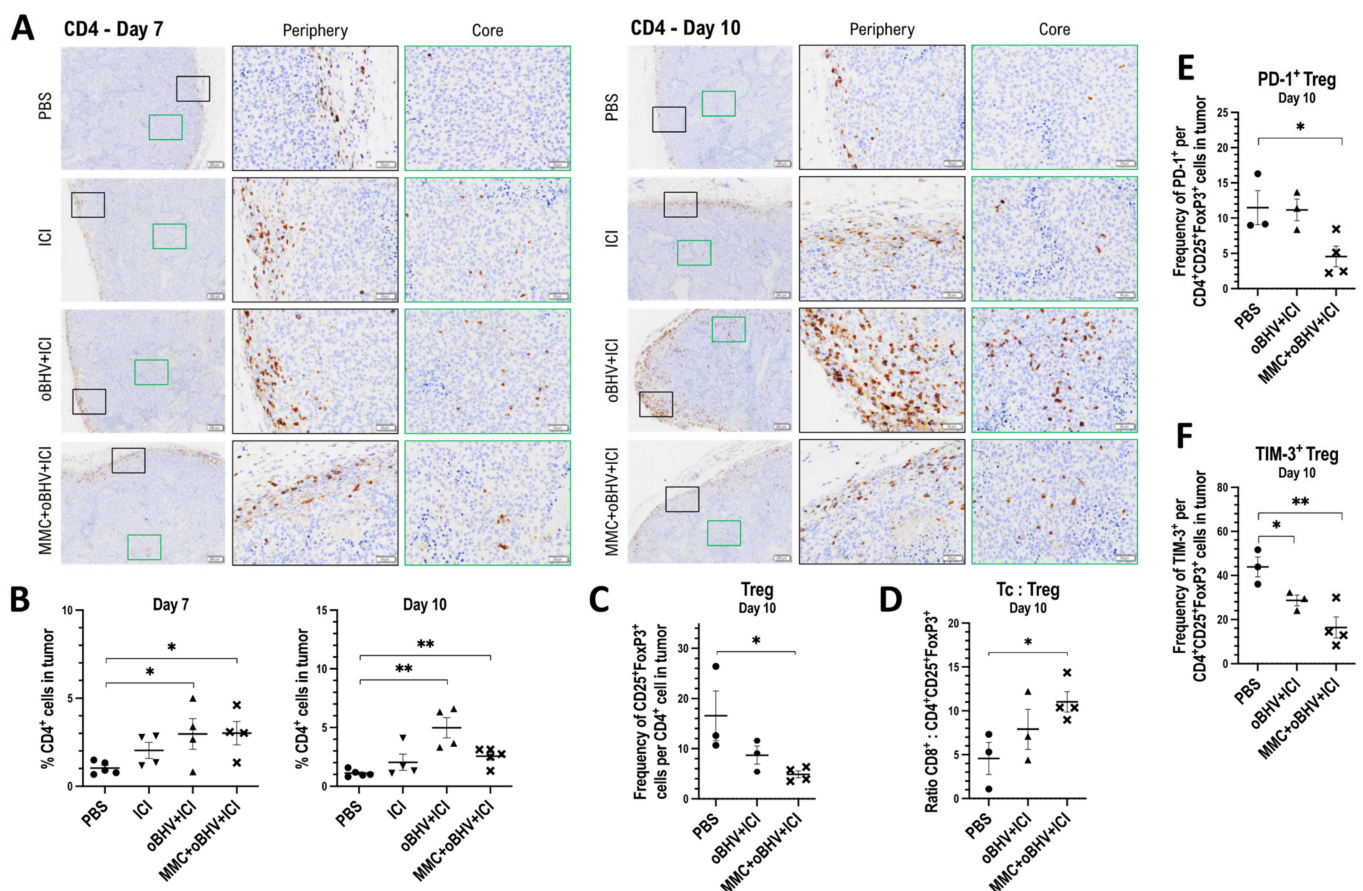


**Figure 5.** B16-C10 tumors were treated with PBS, ICI, oBHV + ICI or MMC + oBHV + ICI. CD4 IHC was performed on tumors on days 7 and 10 (A). Images with 2× magnification are shown in left panels, and 10× images of the tumor periphery (black) and core (green) are shown in the center and right panels. Scale bars: 200 μm (left panels); 50 μm (center and right panels). Quantification of CD4<sup>+</sup> cells was performed over the whole tumor area (B). In addition, tumors were processed on day 10 and TILs were stained for analysis via flow cytometry to determine Treg TILs (C), ratio Tc: Treg (D) and level of activation of Treg TILs. \*  $p < 0.05$ , \*\*  $p < 0.01$ .

### 3.5. Addition of MMC to oBHV Induces Early Release of Anti-Tumor Cytokines and Alters the Tumor Microenvironment

To better understand the role of MMC in combination therapy, tumors treated with PBS, oBHV or MMC + oBHV were harvested and processed for cytokine quantification at early timepoints (Figure 6A and Figure S6). One day after the administration of the first dose of oBHV (day 3), oBHV monotherapy induced the production of IL-6 and MCP-1, two pro-tumoral cytokines, LIF and VEGF, and the anti-tumoral cytokine IP-10. The

addition of low-dose MMC increased the number of cytokines produced, including GM-CSF, TNF $\alpha$ , MIP-1a, MIP-1b and RANTES, five cytokines with reported anti-tumoral properties (Figure 6B). By day 5, monotherapy induced a wider array of cytokines with varied functions but mainly pro-tumoral, while combination therapy did not alter the number of cytokines produced, but their profile (Figure 6C).

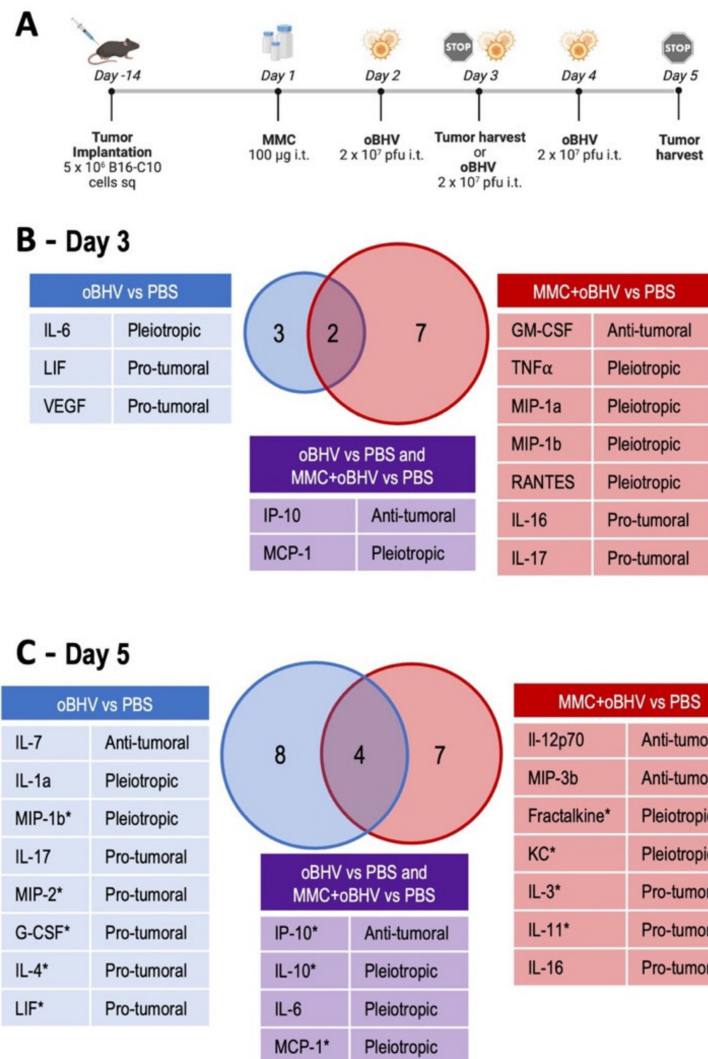


**Figure 6.** Cytokine analysis of tumors treated with PBS, oBHV or MMC + oBHV. On days 3 and 5, tumors were harvested and processing for cytokine quantification via Mouse Cytokine 44-Plex Discovery Assay (A). Venn diagrams represent the number of cytokines in treated tumors on day 3 (B) and day 5 (C) whose levels were significantly increased compared to PBS-treated tumors ( $p < 0.05$ ). Each upregulated cytokine is shown with its reported function in cancer [47–55]. \* indicates the cytokines that were reported to regulate production, activation or recruitment of myeloid cells [56–64]. MIP-1a = CCL3, MIP-1b = CCL4, RANTES = CCL5, IP-10 = CXCL10, MCP-1 = CCL2, Fractalkine = CX3CL1, MIP-2 = CXCL2, MIP-3b = CCL19, KC = CXCL1.

To further explore the mechanism of action upon addition of MMC to oBHV therapy, an unbiased transcriptional profiling was conducted on B16-C10 tumors treated with PBS, oBHV or MMC + oBHV harvested at day 5 (Figures 6A and 7). Unsurprisingly, oBHV strongly induces the expression of IFN-responsive genes (ISGs) as well as that of other immune stimulators, including known anti-viral responders. With addition of MMC, the immune response shifts relative to PBS-treated tumors. Notably, the induction of ISGs (Ifit3, Ifit3b, Ifit1, Ifi44, Oasl2, Usp18, Isg15 and Ddx58) is lower upon addition of MMC, while

genes involved in other responses, such as *Sifn4*, *Plac8*, *Ccl5* and *Ly6c2*, are upregulated to a greater extent (Figure 7A). Furthermore, the addition of MMC to oBHV induces a suite of gene-regulating processes, such as homeostasis, cell cycle progression, antigen presentation and the myeloid lineage, that are not induced in control or oBHV-treated tumors (Figure 7B). Of interest, the cytokine pattern at day 5 showed several cytokines upregulated by both oBHV and MMC + oBHV with reported ability to regulate myeloid cells (Figure 6C marked with \*). These data suggest that MMC both modulates the inflammatory response induced by oBHV and synergizes with oBHV to induce new transcriptional responses which may contribute to the observed efficacy.

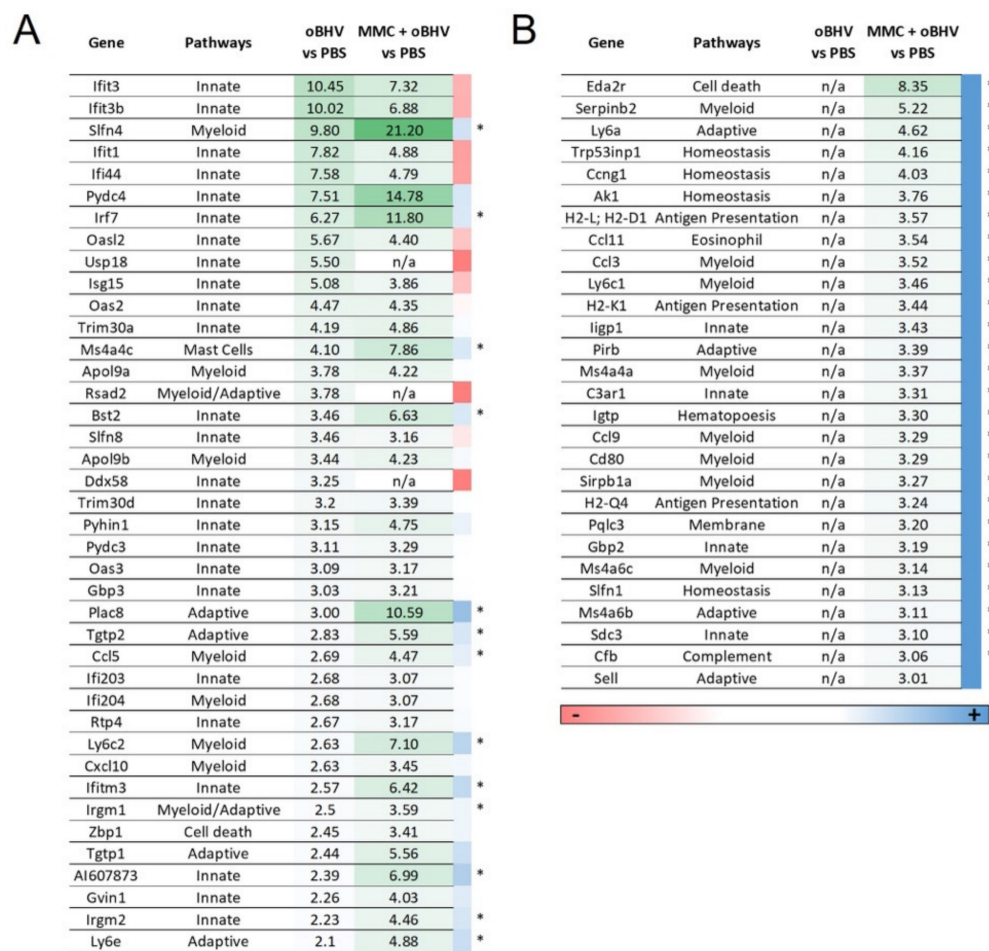


**Figure 7.** Transcriptional profiling of B16-C10 tumors treated with PBS, oBHV or MMC + oBHV showing trends in changes in expression with treatment. (A) Genes significantly upregulated by oBHV expressed as fold expression over PBS, compared to observed fold changes in MMC + oBHV treatment. (B) Genes significantly upregulated by MMC + oBHV expressed as fold expression over PBS that are not upregulated by oBHV alone. Genes suppressed or enhanced by addition of MMC indicated via color scale (red—suppressed, blue—enhanced). \* indicates significant difference when signal data is compared directly ( $p < 0.05$ ).

#### 4. Discussion

While BHV-1 has previously been investigated as an OV [2,21,22,26,27,65,66], here, we validate the first immune competent murine cancer model for pre-clinical analysis of BHV-1. The use of immune competent animal models is imperative for studying OVs since the involvement of the host immune system is essential for OV therapy [4,5,45,46].

Despite immunotherapies showing promising results in clinical trials, one of the biggest limitations remains the highly immune suppressive nature of several cancer types. In this sense, induction of tumor ICD becomes incredibly important to reshape the tumor

immune microenvironment by creating an inflammatory TME conducive for optimal antigen presentation and T cell activation [5,36,44,67–69]. In response to certain chemotherapies, UV radiation and OVs, tumors can undergo ICD [10,11]. We have previously reported that oncolytic HSV-1 (oHSV) requires combination with low-dose MMC, a non-ICD-inducer on its own, to induce bona fide ICD [14]. In addition, with oHSV, we consistently see a correlation between the induction of ICD, TILs and the therapeutic synergy of oHSV with ICI [13,15,16]. In contrast, we show here that oBHV alone is sufficient to induce ICD and activate tumor-specific CD8<sup>+</sup> T cells in peripheral blood even when its in vitro replication is very low. The addition of MMC does not influence either event despite damping the de novo oBHV production in vitro and oBHV-mediated cell death being kinetically slower than MMC + oBHV treatment. While some tumors escape therapeutic pressures by down-regulating the therapeutic target [70,71], given that oBHV replication is limited within treated B16-C10 cells, it is unlikely that oBHV-mediated downregulation of hNectin-1 accounts for the observed efficacy of combination therapy.

Regardless of oBHV inducing bona fide ICD, the addition of MMC is required for oBHV synergy with ICI. Histology of the immune TME revealed that both oBHV and MMC + oBHV combined with ICI induce similar recruitment of CD8<sup>+</sup> TILs with similar activation and exhaustion levels by day 10, despite higher levels with triple combination at day 7. Histology of CD4<sup>+</sup> TILs showed a different situation. Tumors treated with oBHV + ICI presented higher CD4<sup>+</sup> TIL levels than triple combination; subsequent flow cytometry analysis revealed that only the triple combination significantly reduced the proportion of Tregs, increasing the Tc:Treg ratio. In particular, triple combination therapy decreases the proportion of highly suppressive PD-1<sup>+</sup> Tregs. In accordance with ref. [72], these findings suggest a regulatory function of MMC in trafficking and activating Tregs in B16-C10 tumors. With that in mind, the insertion of different therapeutic entities into the virus backbone to provide functions that MMC provides, such as reprogramming Tregs into activated T helper cells [73–75], may be a strategic way to improve oBHV therapeutic efficacy and simplify the treatment modality.

To better understand what is happening in the TME after treatment with our combination strategies, we performed a cytokine analysis and transcriptional profiling. Neither the cytokine analysis nor the transcriptional profiling showed any pattern that can fully explain the correlation between the addition of MMC and Treg regulation. However, the cytokine pattern clearly showed a shift towards a more anti-tumoral TME upon addition of MMC, with upregulation of GM-CSF, TNF- $\alpha$ , MIP-1a, MIP-1b and RANTES at day 3, and IL-12p70, MIP-3b, Fractalkine and KC at day 5 [47,49,50,53,54]. Moreover, only tumors treated with oBHV monotherapy presented high levels of LIF. LIF can regulate CXCL9 in tumor-associated macrophages and prevent tumor infiltration of CD8<sup>+</sup> T cells [48], explaining the slower CD8<sup>+</sup> TILs kinetics seen with oBHV + ICI.

In addition, the cytokine pattern in the TME can potentially be used as biomarker of ICD [55]. OV-mediated ICD triggers the release of IL-6, IL-8, IFN- $\beta$ , IP-10 (CXCL10), MCP-1 (CCL2) and KC (CXCL1) from cancer cells to recruit different immune cells and initiate an anti-tumor response [54,55,76,77]. As seen with the gold standard ICD assay, oBHV alone is sufficient to upregulate three ICD-related cytokines (IL-6, IP-10 and MCP-1). The addition of MMC only affects oBHV-induced IL-6 production at day 3 and upregulates KC at day 5. In contrast to our findings, IL-6 participates in the differentiation of naïve CD4<sup>+</sup> T cells into Th17 while inhibiting their orientation toward the Tregs lineage [78], and increased levels of KC are associated with the recruitment of Treg to tumors [79]. However, both cytokines have pleiotropic properties: IL-6 is also related with pro-tumoral functions such as activation of carcinogenesis and tumor outgrowth, mediation of cytokine release syndrome and promotion of cachexia [47], and KC helps to recruit other immune cells, such as T cells and neutrophils, that can contribute to tumor control [80].

The transcriptional profiling showed that oBHV, as expected, induces a strong up-regulation of several ISGs and other genes involved in the host anti-viral response. The addition of MMC causes a downregulation of some oBHV-upregulated ISGs (Ifit3, Ifit3b,

Ifi1, Ifi44, Oasl2, Usp18, Isg15 and Ddx58) and an upregulation of genes involved in different pathways, including myeloid cell regulation (Slfn4, Ccl5, Ly6c2, Irgm1). Moreover, we found that only the combination MMC + oBHV upregulates another set of genes involved in myeloid pathways (Serpib2, Ccl3, Ly6c1, Ms4a4a, Ccl9, Cd80, Sirb1a and Ms4a6c). Myeloid cells are among the most important defenders against infection, but they are also essential in tissue homeostasis and regulating T cell immunity [81]. In the context of cancer, myeloid cells have a controversial role in modulating tumor responses to various treatments [82]. In the case of oncolytic virotherapy, it has been reported that several OV, including HSV-1, stimulate the release of a plethora of pro-inflammatory cytokines to recruit and activate myeloid cells and their differentiation into inflammatory (M1) macrophages or dendritic cells which engulf dying malignant cells and cross-present TAAs to naïve T cells [55]. Our cytokine analysis and transcriptional profiling also reflect the important role of myeloid cells in oBHV's mechanism of action.

## 5. Conclusions

This study describes the first pre-clinical immune competent mouse model of cancer to evaluate the efficacy of oncolytic BHV-1. Despite being an alpha-herpesvirus akin to HSV-1, BHV-1 has many distinct properties that suggest its widespread and efficacious use as an oncolytic virus. Here, we show that oBHV is sufficient to induce bona fide ICD within immune cold melanoma tumors, resulting in the influx of CD4<sup>+</sup> and CD8<sup>+</sup> TILs. The addition of low-dose MMC chemotherapy does not enhance the immunogenicity of the treatment per se, distinct from its role with oHSV-1, but appears to shift the immune response from predominantly anti-viral, as evidenced by a high level of ISGs, to one that stimulates myeloid cells, antigen presentation and adaptive processes instead. This shift in the tumor microenvironment is critical to sensitize tumors to treatment with ICI, in part through the dampening of suppressive Tregs. These findings will enable the development of oBHV vectors expressing strategic transgenes to optimize clinical efficacy.

**Supplementary Materials:** The following supporting information can be downloaded at: <https://www.mdpi.com/article/10.3390/cancers15041295/s1>, Figure S1: Evaluating optimal conditions for ICD gold standard assay; Figure S2: Expression of human nectin-1 (hNectin-1) increases the susceptibility of B16 cells to oBHV; Figure S3: Low-productive infection of oBHV in B16-C10 cells fails to explain low efficacy as monotherapy; Figure S4: MMC significantly dampens the production of new oBHV particles without altering B16-C10 viability; Figure S5: Efficacy of oBHV alone or in combination with MMC as an infected-cell vaccine; Figure S6: Effect of oBHV treatment with or without MMC on cytokine production in B16-C10 tumors.

**Author Contributions:** Conceptualization, M.E.D. and K.M.; methodology, M.E.D., S.C., O.S., S.R. and K.M.; validation, M.E.D., O.C. and S.R.; formal analysis, M.E.D. and O.C.; investigation, M.E.D., O.C., A.V., N.E.-S., S.C., O.S. and S.R.; resources, K.A., Y.W. and K.M.; writing—original draft preparation, M.E.D. and O.C.; writing—review and editing, M.E.D., O.C., A.V., N.E.-S., S.C., O.S., S.R., K.A., Y.W. and K.M.; visualization, M.E.D. and O.C.; supervision, M.E.D., K.A., Y.W. and K.M.; project administration, M.E.D. and K.M.; funding acquisition, M.E.D. and K.M. All authors have read and agreed to the published version of the manuscript.

**Funding:** This research was funded by the Cancer Research Society, grant number 21170, the Canadian Institutes for Health Research, grant number PJT-178174 and the Canadian Cancer Society, grant number 706280. The APC was funded by the Canadian Institutes for Health Research, grant number PJT-178174.

**Institutional Review Board Statement:** The animal study protocol was approved by the Animal Research Ethics Board of McMaster University (Animal Utilization Protocols 17-05-22 and 21-02-11 approved on 4 July 2017 and 19 April 2021, respectively).

**Informed Consent Statement:** Not applicable.

**Data Availability Statement:** Clariom S assay data (Figure 7) can be found in the GEO database (GSE223637).

**Acknowledgments:** We thank Gary Cohen (University of Pennsylvania, USA) and Günther Keil (Friedrich-Loeffler-Institut, Germany) for reagents, and Mary Jo Smith and Mary Bruni (McMaster Immunology Research Centre Histology Facility, Canada) for histology services. Timelines and schedules were created with BioRender.com (accessed on 12 February 2023).

**Conflicts of Interest:** The authors declare no conflict of interest.

## References

1. Lemay, C.G.; Keller, B.A.; Edge, R.E.; Abei, M.; Bell, J.C. Oncolytic Viruses: The Best is Yet to Come. *Curr. Cancer Drug Targets* **2018**, *18*, 109–123. [[CrossRef](#)] [[PubMed](#)]
2. Cuddington, B.P.; Dyer, A.L.; Workenhe, S.T.; Mossman, K.L. Oncolytic bovine herpesvirus type 1 infects and kills breast tumor cells and breast cancer-initiating cells irrespective of tumor subtype. *Cancer Gene* **2013**, *20*, 282–289. [[CrossRef](#)] [[PubMed](#)]
3. Zeng, W.; Hu, P.; Wu, J.; Wang, J.; Li, J.; Lei, L.; Liu, R. The oncolytic herpes simplex virus vector G47 effectively targets breast cancer stem cells. *Oncol. Rep.* **2013**, *29*, 1108–1114. [[CrossRef](#)] [[PubMed](#)]
4. Workenhe, S.T.; Mossman, K.L. Oncolytic virotherapy and immunogenic cancer cell death: Sharpening the sword for improved cancer treatment strategies. *Mol. Ther.* **2014**, *22*, 251–256. [[CrossRef](#)]
5. Workenhe, S.T.; Verschoor, M.L.; Mossman, K.L. The role of oncolytic virus immunotherapies to subvert cancer immune evasion. *Future Oncol.* **2015**, *11*, 675–689. [[CrossRef](#)]
6. Pol, J.G.; Levesque, S.; Workenhe, S.T.; Gujar, S.; Le Boeuf, F.; Clements, D.R.; Fahrner, J.E.; Fend, L.; Bell, J.C.; Mossman, K.; et al. Trial Watch: Oncolytic viro-immunotherapy of hematologic and solid tumors. *Oncoimmunology* **2018**, *7*, e1503032. [[CrossRef](#)]
7. Locy, H.; de Mey, S.; de Mey, W.; De Ridder, M.; Thielemans, K.; Maenhout, S.K. Immunomodulation of the Tumor Microenvironment: Turn Foe Into Friend. *Front. Immunol.* **2018**, *9*, 2909. [[CrossRef](#)]
8. Raja, J.; Ludwig, J.M.; Gettinger, S.N.; Schalper, K.A.; Kim, H.S. Oncolytic virus immunotherapy: Future prospects for oncology. *J. Immunother. Cancer* **2018**, *6*, 140. [[CrossRef](#)]
9. Gujar, S.; Pol, J.G.; Kroemer, G. Heating it up: Oncolytic viruses make tumors ‘hot’ and suitable for checkpoint blockade immunotherapies. *Oncoimmunology* **2018**, *7*, e1442169. [[CrossRef](#)]
10. Galluzzi, L.; Buque, A.; Kepp, O.; Zitvogel, L.; Kroemer, G. Immunogenic cell death in cancer and infectious disease. *Nat. Rev. Immunol.* **2017**, *17*, 97–111. [[CrossRef](#)]
11. Guo, Z.S.; Liu, Z.; Bartlett, D.L. Oncolytic Immunotherapy: Dying the Right Way is a Key to Eliciting Potent Antitumor Immunity. *Front. Oncol.* **2014**, *4*, 74. [[CrossRef](#)]
12. Filley, A.C.; Dey, M. Immune System, Friend or Foe of Oncolytic Virotherapy? *Front. Oncol.* **2017**, *7*, 106. [[CrossRef](#)]
13. Workenhe, S.T.; Pol, J.G.; Lichty, B.D.; Cummings, D.T.; Mossman, K.L. Combining oncolytic HSV-1 with immunogenic cell death-inducing drug mitoxantrone breaks cancer immune tolerance and improves therapeutic efficacy. *Cancer Immunol. Res.* **2013**, *1*, 309–319. [[CrossRef](#)]
14. Workenhe, S.T.; Nguyen, A.; Bakhshinyan, D.; Wei, J.; Hare, D.N.; MacNeill, K.L.; Wan, Y.; Oberst, A.; Bramson, J.L.; Nasir, J.A.; et al. De novo necroptosis creates an inflammatory environment mediating tumor susceptibility to immune checkpoint inhibitors. *Commun. Biol.* **2020**, *3*, 645. [[CrossRef](#)]
15. Vito, A.; Salem, O.; El-Sayes, N.; MacFawn, I.P.; Portillo, A.L.; Milne, K.; Harrington, D.; Ashkar, A.A.; Wan, Y.; Workenhe, S.T.; et al. Immune checkpoint blockade in triple negative breast cancer influenced by B cells through myeloid-derived suppressor cells. *Commun. Biol.* **2021**, *4*, 859. [[CrossRef](#)]
16. El-Sayes, N.; Vito, A.; Salem, O.; Workenhe, S.T.; Wan, Y.; Mossman, K. A Combination of Chemotherapy and Oncolytic Virotherapy Sensitizes Colorectal Adenocarcinoma to Immune Checkpoint Inhibitors in a cDC1-Dependent Manner. *Int. J. Mol. Sci.* **2022**, *23*, 1754. [[CrossRef](#)]
17. Warner, S.G.; O’Leary, M.P.; Fong, Y. Therapeutic oncolytic viruses: Clinical advances and future directions. *Curr. Opin. Oncol.* **2017**, *29*, 359–365. [[CrossRef](#)]
18. Ott, P.A.; Hodi, F.S. Talimogene Laherparepvec for the Treatment of Advanced Melanoma. *Clin. Cancer Res.* **2016**, *22*, 3127–3131. [[CrossRef](#)]
19. Martinez-Quintanilla, J.; Seah, I.; Chua, M.; Shah, K. Oncolytic viruses: Overcoming translational challenges. *J. Clin. Investig.* **2019**, *130*, 1407–1418. [[CrossRef](#)]
20. Wong, H.H.; Lemoine, N.R.; Wang, Y. Oncolytic Viruses for Cancer Therapy: Overcoming the Obstacles. *Viruses* **2010**, *2*, 78–106. [[CrossRef](#)]
21. Rodrigues, R.; Cuddington, B.; Mossman, K. Bovine herpesvirus type 1 as a novel oncolytic virus. *Cancer Gene* **2010**, *17*, 344–355. [[CrossRef](#)] [[PubMed](#)]
22. Cuddington, B.P.; Mossman, K.L. Permissiveness of human cancer cells to oncolytic bovine herpesvirus 1 is mediated in part by KRAS activity. *J. Virol.* **2014**, *88*, 6885–6895. [[CrossRef](#)] [[PubMed](#)]
23. Cuddington, B.P.; Mossman, K.L. Oncolytic bovine herpesvirus type 1 as a broad spectrum cancer therapeutic. *Curr. Opin. Virol.* **2015**, *13*, 11–16. [[CrossRef](#)] [[PubMed](#)]
24. Hushur, O.; Takashima, Y.; Matsumoto, Y.; Otsuka, H. Restriction of bovine herpesvirus 1 (BHV-1) growth in non-permissive cells beyond the expression of immediate early genes. *J. Vet. Med. Sci.* **2004**, *66*, 453–455. [[CrossRef](#)]

25. Campadelli-Fiume, G.; Cocchi, F.; Menotti, L.; Lopez, M. The novel receptors that mediate the entry of herpes simplex viruses and animal alphaherpesviruses into cells. *Rev. Med. Virol.* **2000**, *10*, 305–319. [[CrossRef](#)]
26. Cuddington, B.; Verschoor, M.; Mossman, K. Handling of the cotton rat in studies for the pre-clinical evaluation of oncolytic viruses. *J. Vis. Exp.* **2014**, *93*, e52232. [[CrossRef](#)]
27. Cuddington, B.P.; Verschoor, M.; Ashkar, A.; Mossman, K.L. Enhanced efficacy with azacytidine and oncolytic BHV-1 in a tolerized cotton rat model of breast adenocarcinoma. *Mol. Oncolytics* **2015**, *2*, 15004. [[CrossRef](#)]
28. Miller, C.G.; Krummenacher, C.; Eisenberg, R.J.; Cohen, G.H.; Fraser, N.W. Development of a syngenic murine B16 cell line-derived melanoma susceptible to destruction by neuroattenuated HSV-1. *Mol. Ther.* **2001**, *3*, 160–168. [[CrossRef](#)]
29. Spear, P.G.; Eisenberg, R.J.; Cohen, G.H. Three classes of cell surface receptors for alphaherpesvirus entry. *Virology* **2000**, *275*, 1–8. [[CrossRef](#)]
30. Geraghty, R.J.; Krummenacher, C.; Cohen, G.H.; Eisenberg, R.J.; Spear, P.G. Entry of alphaherpesviruses mediated by poliovirus receptor-related protein 1 and poliovirus receptor. *Science* **1998**, *280*, 1618–1620. [[CrossRef](#)]
31. Workman, A.; Jones, C. Productive infection and bICP0 early promoter activity of bovine herpesvirus 1 are stimulated by E2F1. *J. Virol.* **2010**, *84*, 6308–6317. [[CrossRef](#)]
32. Keil, G.M.; Höhle, C.; Giesow, K.; König, P. Engineering glycoprotein B of bovine herpesvirus 1 to function as transporter for secreted proteins: A new protein expression approach. *J. Virol.* **2005**, *79*, 791–799. [[CrossRef](#)]
33. Abu Eid, R.; Razavi, G.S.E.; Mkrtychyan, M.; Janik, J.; Khleif, S.N. Old-School Chemotherapy in Immunotherapeutic Combination in Cancer, A Low-cost Drug Repurposed. *Cancer Immunol. Res.* **2016**, *4*, 377–382. [[CrossRef](#)]
34. Galluzzi, L.; Buqué, A.; Kepp, O.; Zitvogel, L.; Kroemer, G. Immunological Effects of Conventional Chemotherapy and Targeted Anticancer Agents. *Cancer Cell* **2015**, *28*, 690–714. [[CrossRef](#)]
35. Landreneau, J.P.; Shurin, M.R.; Agassandian, M.V.; Keskinov, A.A.; Ma, Y.; Shurin, G.V. Immunological Mechanisms of Low and Ultra-Low Dose Cancer Chemotherapy. *Cancer Microenviron.* **2015**, *8*, 57–64. [[CrossRef](#)]
36. Obeid, M.; Tesniere, A.; Ghiringhelli, F.; Fimia, G.M.; Apetoh, L.; Perfettini, J.L.; Castedo, M.; Mignot, G.; Panaretakis, T.; Casares, N.; et al. Calreticulin exposure dictates the immunogenicity of cancer cell death. *Nat. Med.* **2007**, *13*, 54–61. [[CrossRef](#)]
37. Casares, N.; Pequignot, M.O.; Tesniere, A.; Ghiringhelli, F.; Roux, S.; Chaput, N.; Schmitt, E.; Hamai, A.; Hervas-Stubbs, S.; Obeid, M.; et al. Caspase-dependent immunogenicity of doxorubicin-induced tumor cell death. *J. Exp. Med.* **2005**, *202*, 1691–1701. [[CrossRef](#)]
38. Obeid, M.; Tesniere, A.; Panaretakis, T.; Tufi, R.; Joza, N.; van Endert, P.; Ghiringhelli, F.; Apetoh, L.; Chaput, N.; Flament, C.; et al. Ecto-calreticulin in immunogenic chemotherapy. *Immunol. Rev.* **2007**, *220*, 22–34. [[CrossRef](#)]
39. Simpson, G.R.; Horvath, A.; Annels, N.E.; Pencavel, T.; Metcalf, S.; Seth, R.; Peschard, P.; Price, T.; Coffin, R.S.; Mostafid, H.; et al. Combination of a fusogenic glycoprotein, pro-drug activation and oncolytic HSV as an intravesical therapy for superficial bladder cancer. *Br. J. Cancer* **2012**, *106*, 496–507. [[CrossRef](#)]
40. Mullerad, M.; Bochner, B.H.; Adusumilli, P.S.; Bhargava, A.; Kikuchi, E.; Hui-Ni, C.; Kattan, M.W.; Chou, T.C.; Fong, Y. Herpes simplex virus based gene therapy enhances the efficacy of mitomycin C for the treatment of human bladder transitional cell carcinoma. *J. Urol.* **2005**, *174*, 741–746. [[CrossRef](#)]
41. Bennett, J.J.; Adusumilli, P.; Petrowsky, H.; Burt, B.M.; Roberts, G.; Delman, K.A.; Zager, J.S.; Chou, T.C.; Fong, Y. Up-regulation of GADD34 mediates the synergistic anticancer activity of mitomycin C and a  $\gamma$ 134.5 deleted oncolytic herpes virus (G207). *FASEB J.* **2004**, *18*, 1001–1003. [[CrossRef](#)] [[PubMed](#)]
42. Toyozumi, T.; Mick, R.; Abbas, A.E.; Kang, E.H.; Kaiser, L.R.; Molnar-Kimber, K.L. Combined therapy with chemotherapeutic agents and herpes simplex virus type 1 ICP34.5 mutant (HSV-1716) in human non-small cell lung cancer. *Hum. Gene* **1999**, *10*, 3013–3029. [[CrossRef](#)] [[PubMed](#)]
43. Workenhe, S.T.; Simmons, G.; Pol, J.G.; Lichty, B.D.; Halford, W.P.; Mossman, K.L. Immunogenic HSV-mediated oncolysis shapes the antitumor immune response and contributes to therapeutic efficacy. *Mol. Ther.* **2014**, *22*, 123–131. [[CrossRef](#)] [[PubMed](#)]
44. Kepp, O.; Senovilla, L.; Vitale, I.; Vacchelli, E.; Adjemian, S.; Agostinis, P.; Apetoh, L.; Aranda, F.; Barnaba, V.; Bloy, N.; et al. Consensus guidelines for the detection of immunogenic cell death. *Oncoimmunology* **2014**, *3*, e955691. [[CrossRef](#)] [[PubMed](#)]
45. Van Vloten, J.P.; Workenhe, S.T.; Wootton, S.K.; Mossman, K.L.; Bridle, B.W. Critical Interactions between Immunogenic Cancer Cell Death, Oncolytic Viruses, and the Immune System Define the Rational Design of Combination Immunotherapies. *J. Immunol.* **2018**, *200*, 450–458. [[CrossRef](#)]
46. Davola, M.E.; Mossman, K.L. Oncolytic viruses: How “lytic” must they be for therapeutic efficacy? *Oncoimmunology* **2019**, *8*, e1581528. [[CrossRef](#)]
47. Briukhovetska, D.; Dörr, J.; Endres, S.; Libby, P.; Dinarello, C.A.; Kobold, S. Interleukins in cancer: From biology to therapy. *Nat. Rev. Cancer* **2021**, *21*, 481–499. [[CrossRef](#)]
48. Pascual-García, M.; Bonfill-Teixidor, E.; Planas-Rigol, E.; Rubio-Perez, C.; Iurlaro, R.; Arias, A.; Cuartas, I.; Sala-Hojman, A.; Escudero, L.; Martínez-Ricarte, F.; et al. LIF regulates CXCL9 in tumor-associated macrophages and prevents CD8(+) T cell tumor-infiltration impairing anti-PD1 therapy. *Nat. Commun.* **2019**, *10*, 2416. [[CrossRef](#)]
49. Berraondo, P.; Sanmamed, M.F.; Ochoa, M.C.; Etxeberria, I.; Aznar, M.A.; Pérez-Gracia, J.L.; Rodríguez-Ruiz, M.E.; Ponz-Sarvisé, M.; Castañón, E.; Melero, I. Cytokines in clinical cancer immunotherapy. *Br. J. Cancer* **2019**, *120*, 6–15. [[CrossRef](#)]
50. Adams, R.; Moser, B.; Karagiannis, S.N.; Lacy, K.E. Chemokine Pathways in Cutaneous Melanoma: Their Modulation by Cancer and Exploitation by the Clinician. *Cancers* **2021**, *13*, 5625. [[CrossRef](#)]



51. Karagiannidis, I.; Salataj, E.; Said Abu Egal, E.; Beswick, E.J. G-CSF in tumors: Aggressiveness, tumor microenvironment and immune cell regulation. *Cytokine* **2021**, *142*, 155479. [[CrossRef](#)]
52. Kamran, N.; Li, Y.; Sierra, M.; Alghamri, M.S.; Kadiyala, P.; Appelman, H.D.; Edwards, M.; Lowenstein, P.R.; Castro, M.G. Melanoma induced immunosuppression is mediated by hematopoietic dysregulation. *Oncimmunology* **2018**, *7*, e1408750. [[CrossRef](#)]
53. Nagarsheth, N.; Wicha, M.S.; Zou, W. Chemokines in the cancer microenvironment and their relevance in cancer immunotherapy. *Nat. Rev. Immunol.* **2017**, *17*, 559–572. [[CrossRef](#)]
54. Pol, J.G.; Workenhe, S.T.; Konda, P.; Gujar, S.; Kroemer, G. Cytokines in oncolytic virotherapy. *Cytokine Growth Factor Rev.* **2020**, *56*, 4–27. [[CrossRef](#)]
55. Galluzzi, L.; Vitale, I.; Warren, S.; Adjemian, S.; Agostinis, P.; Martinez, A.B.; Chan, T.A.; Coukos, G.; Demaria, S.; Deutsch, E.; et al. Consensus guidelines for the definition, detection and interpretation of immunogenic cell death. *J. ImmunoTher. Cancer* **2020**, *8*, e000337. [[CrossRef](#)]
56. Greene, J.T.; Brian, B.F.t.; Senevirathne, S.E.; Freedman, T.S. Regulation of myeloid-cell activation. *Curr. Opin. Immunol.* **2021**, *73*, 34–42. [[CrossRef](#)]
57. Gabrilovich, D.I.; Ostrand-Rosenberg, S.; Bronte, V. Coordinated regulation of myeloid cells by tumours. *Nat. Rev. Immunol.* **2012**, *12*, 253–268. [[CrossRef](#)]
58. Jorgensen, M.M.; de la Puente, P. Leukemia Inhibitory Factor: An Important Cytokine in Pathologies and Cancer. *Biomolecules* **2022**, *12*, 217. [[CrossRef](#)]
59. Kusmartsev, S.; Gabrilovich, D.I. Effect of tumor-derived cytokines and growth factors on differentiation and immune suppressive features of myeloid cells in cancer. *Cancer Metastasis Rev.* **2006**, *25*, 323–331. [[CrossRef](#)]
60. Kumar, A.H.; Martin, K.; Turner, E.C.; Buneker, C.K.; Dorgham, K.; Deterre, P.; Caplice, N.M. Role of CX3CR1 receptor in monocyte/macrophage driven neovascularization. *PLoS ONE* **2013**, *8*, e57230. [[CrossRef](#)]
61. Marchica, V.; Toscani, D.; Corcione, A.; Bolzoni, M.; Storti, P.; Vescovini, R.; Ferretti, E.; Dalla Palma, B.; Vicario, E.; Accardi, F.; et al. Bone Marrow CX3CL1/Fractalkine is a New Player of the Pro-Angiogenic Microenvironment in Multiple Myeloma Patients. *Cancers* **2019**, *11*, 321. [[CrossRef](#)] [[PubMed](#)]
62. Hu, J.; Zhao, Q.; Kong, L.Y.; Wang, J.; Yan, J.; Xia, X.; Jia, Z.; Heimberger, A.B.; Li, S. Regulation of tumor immune suppression and cancer cell survival by CXCL1/2 elevation in glioblastoma multiforme. *Sci. Adv.* **2021**, *7*, eabc2511. [[CrossRef](#)] [[PubMed](#)]
63. Sumida, K.; Ohno, Y.; Ohtake, J.; Kaneumi, S.; Kishikawa, T.; Takahashi, N.; Taketomi, A.; Kitamura, H. IL-11 induces differentiation of myeloid-derived suppressor cells through activation of STAT3 signalling pathway. *Sci. Rep.* **2015**, *5*, 13650. [[CrossRef](#)] [[PubMed](#)]
64. Magidey-Klein, K.; Cooper, T.J.; Kveler, K.; Normand, R.; Zhang, T.; Timaner, M.; Raviv, Z.; James, B.P.; Gazit, R.; Ronai, Z.e.A.; et al. IL-6 contributes to metastatic switch via the differentiation of monocytic-dendritic progenitors into prometastatic immune cells. *J. ImmunoTher. Cancer* **2021**, *9*, e002856. [[CrossRef](#)]
65. Ding, X.; Yuan, W.; Yang, H.; Liu, C.; Li, S.; Zhu, L.  $\beta$ -Catenin-Specific Inhibitor, iCRT14, Promotes BoHV-1 Infection-Induced DNA Damage in Human A549 Lung Adenocarcinoma Cells by Enhancing Viral Protein Expression. *Int. J. Mol. Sci.* **2022**, *23*, 2328. [[CrossRef](#)]
66. Zhu, L.; Fu, X.; Yuan, C.; Jiang, X.; Zhang, G. Induction of Oxidative DNA Damage in Bovine Herpesvirus 1 Infected Bovine Kidney Cells (MDBK Cells) and Human Tumor Cells (A549 Cells and U2OS Cells). *Viruses* **2018**, *10*, 393. [[CrossRef](#)]
67. Martins, I.; Wang, Y.; Michaud, M.; Ma, Y.; Sukkurwala, A.Q.; Shen, S.; Kepp, O.; Metivier, D.; Galluzzi, L.; Perfettini, J.L.; et al. Molecular mechanisms of ATP secretion during immunogenic cell death. *Cell Death Differ.* **2014**, *21*, 79–91. [[CrossRef](#)]
68. Yang, H.; Wang, H.; Chavan, S.S.; Andersson, U. High Mobility Group Box Protein 1 (HMGB1): The Prototypical Endogenous Danger Molecule. *Mol. Med.* **2015**, *21* (Suppl. S1), S6–S12. [[CrossRef](#)]
69. Garg, A.D.; Galluzzi, L.; Apetoh, L.; Baert, T.; Birge, R.B.; Bravo-San Pedro, J.M.; Breckpot, K.; Brough, D.; Chaurio, R.; Cirone, M.; et al. Molecular and Translational Classifications of DAMPs in Immunogenic Cell Death. *Front. Immunol.* **2015**, *6*, 588. [[CrossRef](#)]
70. Groeneveldt, C.; Kinderman, P.; van den Wollenberg, D.J.M.; van den Oever, R.L.; Middelburg, J.; Mustafa, D.A.M.; Hoeben, R.C.; van der Burg, S.H.; van Hall, T.; van Montfoort, N. Preconditioning of the tumor microenvironment with oncolytic reovirus converts CD3-bispecific antibody treatment into effective immunotherapy. *J. ImmunoTher. Cancer* **2020**, *8*, e001191. [[CrossRef](#)]
71. Bhatt, D.K.; Chammas, R.; Daemen, T. Resistance Mechanisms Influencing Oncolytic Virotherapy, a Systematic Analysis. *Vaccines* **2021**, *9*, 1166. [[CrossRef](#)]
72. Chen, F.Y.-S.; Chi, C.-W.; Shieh, H.-R.; Lin, C.-P.; Ko, C.-C.; Chung, Y.-C.; Lai, J.C.-Y.; Tai, H.-C.; Chen, Y.-J. Mitomycin C modulates tumor microenvironment and enhances radiosensitivity in rectal cancer. *Ther. Radiol. Oncol.* **2019**, *3*, 29. [[CrossRef](#)]
73. Han, S.; Toker, A.; Liu, Z.Q.; Ohashi, P.S. Turning the Tide Against Regulatory T Cells. *Front. Oncol.* **2019**, *9*, 279. [[CrossRef](#)]
74. Wang, D.; Quiros, J.; Mahuron, K.; Pai, C.C.; Ranzani, V.; Young, A.; Silveria, S.; Harwin, T.; Abnousian, A.; Pagani, M.; et al. Targeting EZH2 Reprograms Intratumoral Regulatory T Cells to Enhance Cancer Immunity. *Cell Rep.* **2018**, *23*, 3262–3274. [[CrossRef](#)]
75. Paluskievicz, C.M.; Cao, X.; Abdi, R.; Zheng, P.; Liu, Y.; Bromberg, J.S. T Regulatory Cells and Priming the Suppressive Tumor Microenvironment. *Front. Immunol.* **2019**, *10*, 2453. [[CrossRef](#)]
76. Showalter, A.; Limaye, A.; Oyer, J.L.; Igarashi, R.; Kittipatarin, C.; Copik, A.J.; Khaled, A.R. Cytokines in immunogenic cell death: Applications for cancer immunotherapy. *Cytokine* **2017**, *97*, 123–132. [[CrossRef](#)]

77. Donnelly, O.G.; Errington-Mais, F.; Steele, L.; Hadac, E.; Jennings, V.; Scott, K.; Peach, H.; Phillips, R.M.; Bond, J.; Pandha, H.; et al. Measles virus causes immunogenic cell death in human melanoma. *Gene* **2013**, *20*, 7–15. [[CrossRef](#)]
78. Tanaka, T.; Narazaki, M.; Kishimoto, T. IL-6 in inflammation, immunity, and disease. *Cold Spring Harb. Perspect. Biol.* **2014**, *6*, a016295. [[CrossRef](#)]
79. Lv, M.; Xu, Y.; Tang, R.; Ren, J.; Shen, S.; Chen, Y.; Liu, B.; Hou, Y.; Wang, T. miR141–CXCL1–CXCR2 Signaling–Induced Treg Recruitment Regulates Metastases and Survival of Non–Small Cell Lung Cancer. *Mol. Cancer Ther.* **2014**, *13*, 3152–3162. [[CrossRef](#)]
80. Krombach, J.; Hennel, R.; Brix, N.; Orth, M.; Schoetz, U.; Ernst, A.; Schuster, J.; Zuchtriegel, G.; Reichel, C.A.; Bierschenk, S.; et al. Priming anti-tumor immunity by radiotherapy: Dying tumor cell-derived DAMPs trigger endothelial cell activation and recruitment of myeloid cells. *Oncot Immunology* **2019**, *8*, e1523097. [[CrossRef](#)]
81. Engblom, C.; Pfirschke, C.; Pittet, M.J. The role of myeloid cells in cancer therapies. *Nat. Rev. Cancer* **2016**, *16*, 447–462. [[CrossRef](#)] [[PubMed](#)]
82. Neophytou, C.M.; Pierides, C.; Christodoulou, M.I.; Costeas, P.; Kyriakou, T.C.; Papageorgis, P. The Role of Tumor-Associated Myeloid Cells in Modulating Cancer Therapy. *Front. Oncol.* **2020**, *10*, 899. [[CrossRef](#)] [[PubMed](#)]

**Disclaimer/Publisher’s Note:** The statements, opinions and data contained in all publications are solely those of the individual author(s) and contributor(s) and not of MDPI and/or the editor(s). MDPI and/or the editor(s) disclaim responsibility for any injury to people or property resulting from any ideas, methods, instructions or products referred to in the content.